- Surface Chemistry for Molecular Layer Deposition of Organic and Hybrid Organic–Inorganic Polymers
  George, S. M.; Yoon, B.; Dameron, A. A. *Acc. Chem. Res.* **2009**, *42*, 498–508.
  Abstract:

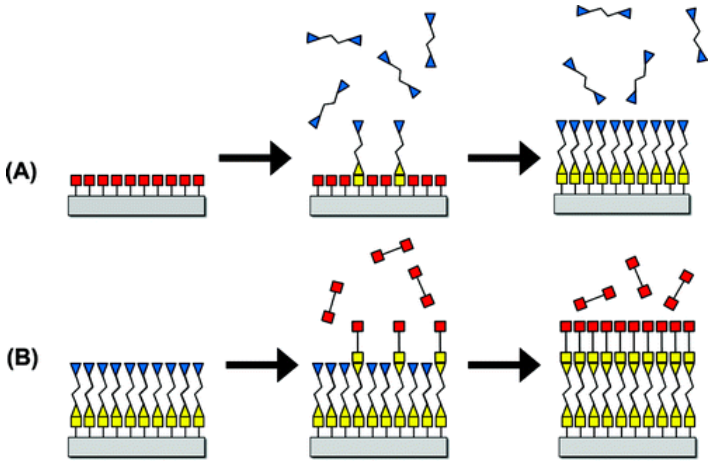

The fabrication of many devices in modern technology requires techniques for growing thin films. As devices miniaturize, manufacturers will need to control thin film growth at the atomic level. Because many devices have challenging morphologies, thin films must be able to coat conformally on structures with high aspect ratios. Techniques based on atomic layer deposition (ALD), a special type of chemical vapor deposition, allow for the growth of ultra-thin and conformal films of inorganic materials using sequential, self-limiting reactions. Molecular layer deposition (MLD) methods extend this strategy to include organic and hybrid organic–inorganic polymeric materials.

In this Account, we provide an overview of the surface chemistry for the MLD of organic and hybrid organic–inorganic polymers and examine a variety of surface chemistry strategies for growing polymer thin films. Previously, surface chemistry for the MLD of organic polymers such as polyamides and polyimides has used two-step AB reaction cycles using homo-bifunctional reactants. However, these reagents can react twice and eliminate active sites on the growing polymer surface. To avoid this problem, we can employ alternative precursors for MLD based on hetero-bifunctional reactants and ring-opening reactions. We can also use surface activation or protected chemical functional groups.

In addition, we can combine the reactants for ALD and MLD to grow hybrid organic–inorganic polymers that should display interesting properties. For example, using trimethylaluminum (TMA) and various diols as reactants, we can achieve the MLD of alucone organic–inorganic polymers. We can alter the chemical and physical properties of these organic–inorganic polymers by varying the organic constituent in the diol or blending the alucone MLD films with purely inorganic ALD films to build a nanocomposite or nanolaminate. The combination of ALD and MLD reactants enlarges the number of possible sequential self-limiting surface reactions for film growth. Extensions to three-step ABC reaction cycles also offer many advantages to avoid the use of homo-bifunctional reactants and incorporate new functionality in the thin film.

The advances in ALD have helped technological development in many areas, including semiconductor processing and magnetic disk-drive manufacturing. We expect that the advances in MLD will lead to innovations in polymeric thin-film products. Although there are remaining challenges, effective surface chemistry strategies are being developed for MLD that offer the opportunity for future advances in materials and device fabrication.

- Enantioselective catalysis with homochiral metal–organic frameworks
  Ma, L.; Abney, C.; Lin, W. *Chem. Soc. Rev.* **2009**, *38*, 1248 – 1256.
  Abstract:

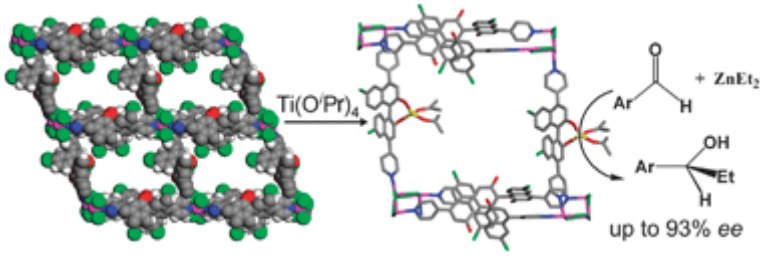

This *tutorial review* presents recent developments of homochiral metal–organic frameworks (MOFs) in enantioselective catalysis. Following a brief introduction of the basic concepts and potential virtues of MOFs in catalysis, we summarize three distinct strategies that have been utilized to synthesize homochiral MOFs. Framework stability and accessibility of the open channels to reagents are then addressed. We finally survey recent successful examples of catalytically active homochiral MOFs based on three approaches, namely, homochiral MOFs with achiral catalytic sites, incorporation of asymmetric catalysts directly into the framework, and post-synthetic modification of homochiral MOFs. Although still in their infancy, homochiral MOFs have clearly demonstrated their utility in heterogeneous asymmetric catalysis, and a bright future is foreseen for the development of practically useful homochiral MOFs in the production of optically pure organic molecules.

- Guided and fluidic self-assembly of microstructures using railed microfluidic channels
  Chung, S. E.; Park, W.; Shin, S.; Lee, S. A.; Kwon, S. *Nature Materials* **2008**, *7*, 581-587.
  Abstract:

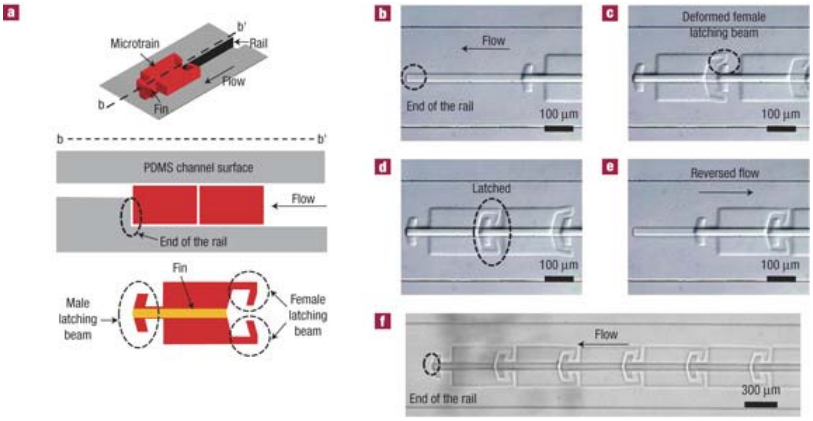

Fluidic self-assembly is a promising pathway for parallel fabrication of devices made up of many small components. Here, we introduce 'railed microfluidics' as an agile method to guide and assemble microstructures inside fluidic channels. The guided movement of microstructures in microfluidic channels was achieved by fabricating grooves ('rails') on the top surface of the channels and also creating complementary polymeric microstructures that fit with the grooves. Using the rails as a guiding mechanism, we built complex one- and two-dimensional microsystems in which all the microstructures initially involved in the fabrication method were incorporated as components in the final product. Complex structures composed of more than 50 microstructures (each sized smaller than 50 µm) were fluidically self-assembled with zero error. Furthermore, we were able to use the rails to guide microstructures through different fluid solutions, successfully overcoming strong interfacial tension between solutions. On the basis of rail-guided self-assembly and cross-solution

movement, we demonstrated heterogeneous fluidic self-assembly of polymeric microstructures and living cells. In addition to such assembly of in situ polymerized structures, we also guided and assembled externally fabricated silicon chips—demonstrating the feasible application of railed microfluidics to other materials systems.

- Surface-structure-regulated cell-membrane penetration by monolayer-protected nanoparticles
  Verma, A.; Uzun, O.; Hu, Y.; Hu, Y.; Han, H.-S.; Watson, N.; Chen, S.; Irvine, D. J.; Stellacci, F. *Nature Materials* **2008**, *7*, 588-595.
  Abstract:

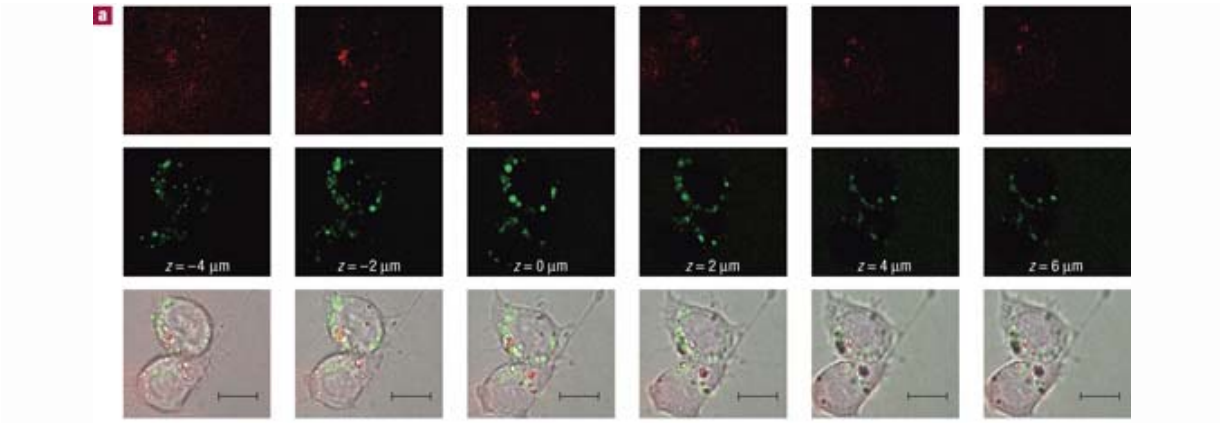

Nanoscale objects are typically internalized by cells into membrane-bounded endosomes and fail to access the cytosolic cell machinery. Whereas some biomacromolecules may penetrate or fuse with cell membranes without overt membrane disruption, no synthetic material of comparable size has shown this property yet. Cationic nano-objects pass through cell membranes by generating transient holes, a process associated with cytotoxicity. Studies aimed at generating cell-penetrating nanomaterials have focused on the effect of size, shape and composition. Here, we compare membrane penetration by two nanoparticle 'isomers' with similar composition (same hydrophobic content), one coated with subnanometre striations of alternating anionic and hydrophobic groups, and the other coated with the same moieties but in a random distribution. We show that the former particles penetrate the plasma membrane without bilayer disruption, whereas the latter are mostly trapped in endosomes. Our results offer a paradigm for analysing the fundamental problem of cell-membrane-penetrating bio- and macro-molecules.

- Cylindrical Superparticles from Semiconductor Nanorods
  Zhuang, J.; Shaller, A. D.; Lynch, J.; Wu, H.; Chen, O.; Li, A. D. Q.; Cao, Y. C. *J. Am. Chem. Soc.* **2009**, *131*, 6084–6085.
  Abstract:

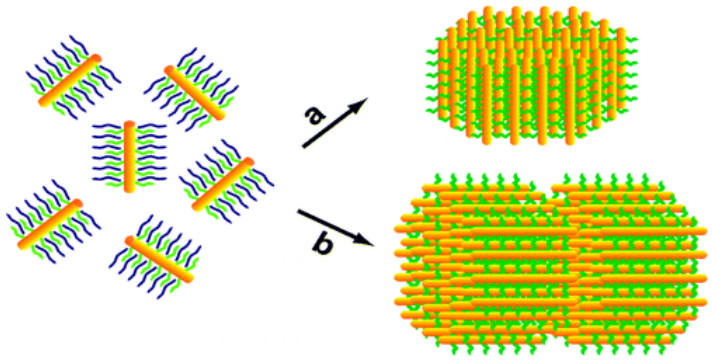

In this communication, we report a synthesis of anisotropic colloidal superparticles (SPs) from CdSe/CdS semiconductor nanorods. These anisotropic SPs are cylindrical disks or stacked-disk arrays. We attribute the major driving forces controlling the SP shape to interparticle interactions between nanorods and solvophobic interactions between a superparticle and its surrounding solvent. According to their sizes (or volumes), the SPs adopt either single- or multilayered structures. In addition, these SPs exhibit linearly polarized emissions, demonstrating their potential role as useful components in devices such as polarized light-emitting diodes and electrooptical modulators.

- High-Performance Air-Stable n-Channel Organic Thin Film Transistors Based on Halogenated Perylene Bisimide Semiconductors
  Schmidt, R.; Oh, J. H.; Sun, Y.; Deppisch, M.; Krause, A. M.; Radacki, K.; Braunschweig, K.; Könemann, M.; Erk, P.; Bao, Z.; Würthner, F. *J. Am. Chem. Soc.* **2009**, *131*, 6215–6228.
  Abstract:

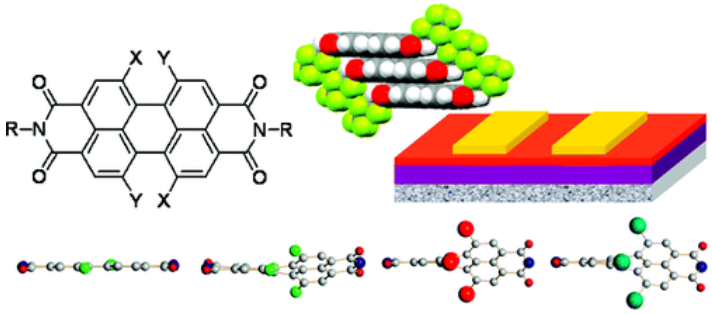

The syntheses and comprehensive characterization of 14 organic semiconductors based on perylene bisimide (PBI) dyes that are equipped with up to four halogen substituents in the bay area of the perylene core and five different highly fluorinated imide substituents are described. The influence of the substituents on the LUMO level and the solid state packing of PBIs was examined by cyclic voltammetry and single crystal structure analyses of seven PBI derivatives, respectively. Top-contact/bottom-gate organic thin film transistor (OTFT) devices were constructed by vacuum deposition of these PBIs on SiO2 gate dielectrics that had been pretreated with n-octadecyl triethoxysilane in vapor phase (OTS-V) or solution phase (OTS-S). The electrical characterization of all devices was accomplished in a nitrogen atmosphere as well as in air, and the structural features of thin films were explored by grazing incidence X-ray diffraction (GIXD) and atomic force microscopy (AFM). Several of those PBIs that bear only hydrogen or up to two fluorine substitutents at the concomitantly flat PBI core afforded excellent n-channel transistors, in particular, on OTS-S substrate and even in air (μ > 0.5 cm2 V−1 s−1; Ion/Ioff > 106). The best OTFTs were obtained for 2,2,3,3,4,4,4-heptafluorobutyl-substituted PBI 1a (“PTCDI-C4F7”) on OTS-S with n-channel field effect mobilities consistently >1 cm2 V−1 s−1 and on-to-off current rations of 106 in a nitrogen atmosphere and in air. For distorted core-tetrahalogenated (fluorine, chlorine, or bromine) PBIs, less advantageous solid

state packing properties were found and high performance OTFTs were obtained from only one tetrachlorinated derivative (2d on OTS-S). The excellent on-to-off current modulation combined with high mobility in air makes these PBIs suitable for a wide range of practical applications.

- Star-Shaped Multichromophoric Arrays from Bodipy Dyes Grafted on Truxene Core
  Diring, S.; Puntoriero, F.; Nastasi, F.; Campagna, S.; Ziessel, R. *J. Am. Chem. Soc.* **2009**, *131*, 6108–6110.
  Abstract:

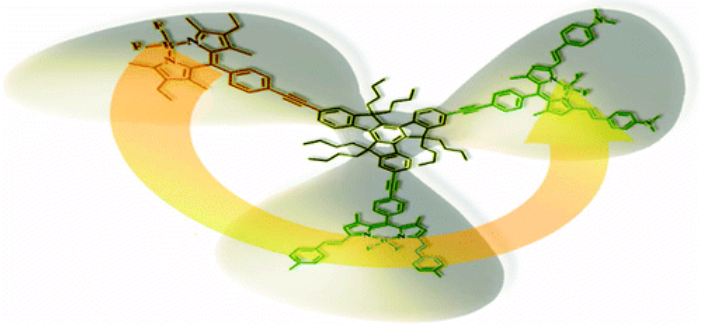

Efficient photoinduced energy migration is obtained in a new star-shaped multichromophoric species made of three different Bodipy dyes and a truxene core.

- Submolecular Observation of Photosensitive Macrocycles and Their Isomerization Effects on Host−Guest Network
  Shen, Y.-T.; Guan, L.; Zhu, X.-Y.; Zeng, Q.-D.; Wang, C. *J. Am. Chem. Soc.* **2009**, *131*, 6174–6180.
  Abstract:

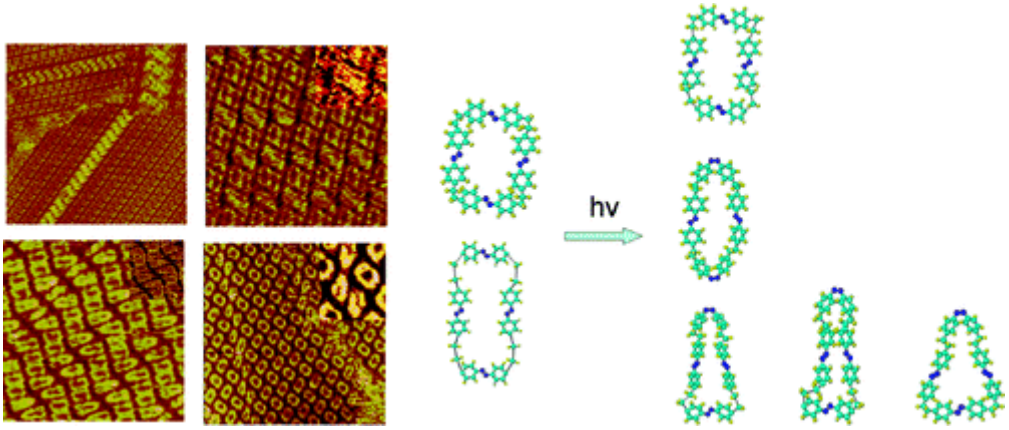

The macrocyclic compounds consisting of photosensitive units as parts of the frame have been extensively studied to mimic photoregulated functions in nature. In this paper, controlled assembly of well-ordered arrays of photosensitive macrocyclic rectangles is demonstrated by using a host−guest molecular template. 4NN-Macrocycle molecules are observed to photoisomerize from trans−trans−trans−trans (t,t,t,t) to a range of isomers including trans−trans−trans−cis (t,t,t,c) and trans−cis−trans−cis (t,c,t,c) isomers after irradiation of UV light. The photoisomers are also observed to affect the guest−host network characteristic appreciably. In the STM observations we can distinguish three (t,t,t,t) conformational isomers, three (t,t,t,c) conformational isomers, and one (t,c,t,c) isomer, which self-assemble into different adlayers with TCDB on a HOPG surface. This study

provides a facile approach to study the photoisomerization processes of the azobenzene groups and the conformational photoisomers.

- Catalytic Growth of Single-Crystalline V_2O_5 Nanowire Arrays
  Velazquez, J. M.; Banerjee, S. *Small* **2009**, *5*, 1025 – 1029.
  Abstract:

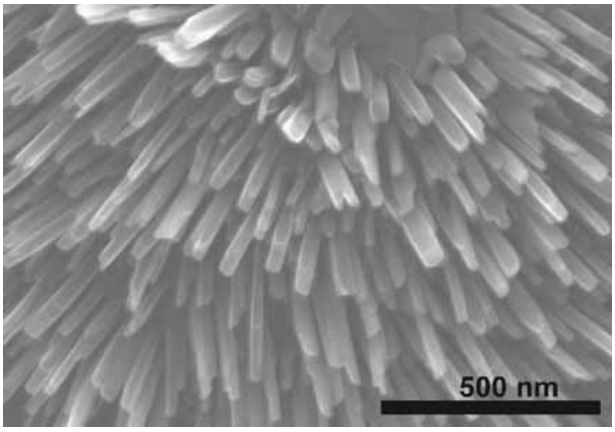

Arrays of V_2O_5 nanowires are grown on silicon substrates by a catalytic vapor-solid mechanism (see image). The obtained nanowires are single-crystalline and highly oriented with their lengths and substrate coverage controlled by the duration of the reaction, reaction temperature, and flow velocity. The growth of these nanowire arrays paves the way for the fabrication of novel battery architectures based on the charging/discharging of individual nanowires.

- Large-Scale Fabrication of 4-nm-Channel Vertical Protein-Based Ambipolar Transistors
  Mentovich, E. D.; Belgorodsky, B.; Kalifa, I.; Cohen, H.; Richter, S. *Nano Lett.* **2009**, *9*, 1296–1300.
  Abstract:

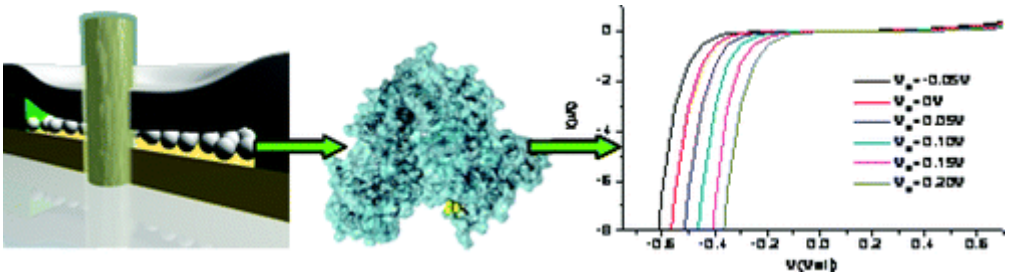

We suggest a universal method for the mass production of nanometer-sized molecular transistors. This vertical-type device was fabricated using conventional photolithography and self-assembly methods and was processed in parallel fashion. We used this transistor to investigate the transport properties of a single layer of bovine serum albumin protein. This 4-nm-channel device exhibits low operating voltages, ambipolar behavior, and high gate sensitivity. The operation mechanism of this new device is suggested, and the charge transfer through the protein layer was explored.

- Molecular tectonics: 3-D organisation of decanuclear silver nanoclusters.
  Kozlova, M. N.; Ferlay, S.; Kyritsakas, N.; Hosseini, M. W.; Solovieva, S. E.; Antipin, I. S.; Konovalov, A. I. *Chem. Commun.* **2009**, 2514 – 2516.
  Abstract :

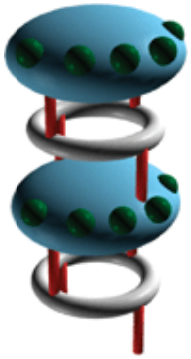

The combination of silver nitrate with a thiacalix[4]arene derivative bearing at the lower rim four benzonitrile groups leads in the crystalline phase to the formation of a 3-D coordination network in which the organic tectons are connected by decanuclear silver nanoclusters.

- Cycloaddition to an anthracene-derived macrocyclic receptor with supramolecular control of regioselectivity.
  Gassensmith, J. J.; Baumes, J. M.; Eberhard, J.; Smith, B. D. *Chem. Commun.* **2009**, 2517 – 2519.
  Abstract:

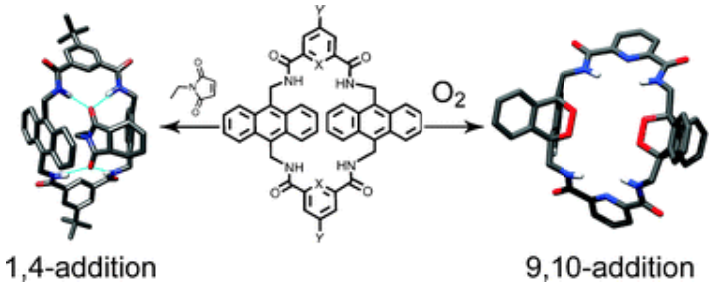

N-Ethylmaleimide and maleic anhydride add to the interior face of one anthracene wall with unusual 1,4-regioselectivity, whereas singlet oxygen adds to both anthracene walls with 9,10-regioselectivity.

- β-Substituted Terthiophene [2]Rotaxanes
  Ikeda, T.; Higuchi, M.; Kurth, D. G. *Chem. Eur. J.* **2009**, *19*, 4906-4913.
  Abstract:

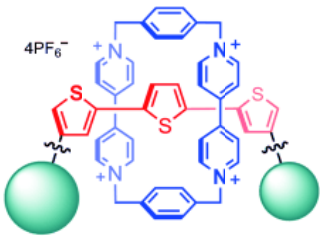

Towards polythiophene polyrotaxanes: The β-substituted terthiophene [2]rotaxanes have been synthesized (see figure). Basic optical and electrochemical properties of the synthesized [2]rotaxanes are also reported.
Two kinds of β-substituted terthiophene [2]rotaxanes were synthesized using the host-guest pairs of the electron-deficient cyclophane cyclobis(paraquat-*p*-phenylene) (**CBPQT**$^{4+}$) and the electron-rich terthiophenes with diethyleneglycol chains at the β-position. One is made from the α-position non-substituted terthiophene (**3 T-β-Rx**) and the other is made from the α-dibromo-substituted terthiophene (**3 TBr-β-Rx**). The binding constants of the β-substituted terthiophene threads were

confirmed to be smaller than that of the α-substituted terthiophene analogue. By UV/Vis absorption measurements, we confirmed the charge-transfer (CT) band in the visible region with an extinction coefficient of $\approx 10^2$ (M^{-1} cm^{-1}). Strong, but not quantitative, quenching of the terthiophene fluorescence was confirmed for the [2]rotaxanes. Although the β-substituted terthiophene thread was electrochemically polymerizable, the [2]rotaxane **3 T-β-Rx** was not polymerizable. This result indicates that the interlocked **CBPQT^{4+}** macrocycle effectively suppresses the electrochemical polymerization of the terthiophene unit because electrostatic repulsive and steric effects of **CBPQT^{4+}** hinder the dimerization of the terthiophene radical cations. In the electrochemical measurement, we confirmed the shift of the first reduction peak towards less negative potential compared to free **CBPQT^{4+}** and the splitting of the second reduction peak. These electrochemical behaviors are similar to those observed for the highly-constrained [2]rotaxanes. The β-substituted terthiophene [2]rotaxanes reported herein are important key compounds to prepare polythiophene polyrotaxanes.

- Cooperative Metal Binding and Helical Folding in Model Peptides of Treble-Clef Zinc Fingers Sénèque, O.; Bonnet, E.; Joumas, F. L.; Latour, J.-M. *Chem. Eur. J.* **2009**, *19*, 4798-4810.
  Abstract:

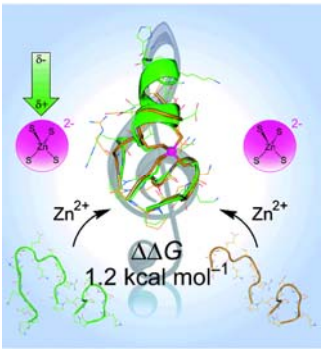

Synergy in zinc fingers: The comparison between peptide folding and metal binding properties of two model peptides of treble-clef zinc fingers presenting high affinities for zinc and cobalt reveals a cooperative effect: the metal folds the peptide into a α-helix, which in turn strengthens the metal core.

Two peptides, L_{TC} and L^{T}_{TC} have been synthesised to model the treble-clef zinc fingers encountered in many $Zn(Cys)_4$-site-containing proteins. Both are cyclic peptides with a linear tail grafted on a glutamate side chain of the cycle. They differ by the length of this tail, which lacks five amino acids in L^{T}_{TC} compared to L_{TC}. Both peptides bind Zn^{2+} and Co^{2+} in 1:1 metal/peptide ratio and the structure of these complexes have been characterised by NMR, UV/Vis and CD spectroscopy. Both peptides fold the same way around the metal ion and they fully reproduce the classical fold of treble-clef zinc fingers and display an extended hydrogen-bond network around the coordinating sulfur atoms. The structures of the $M \cdot L_{TC}$ complexes reveal that the linear tail forms a short two-turn α-helix, present in the metallated form only. The formation of this helix constitutes a rare example of metal-induced folding. The second turn of this helix is composed of the five amino acids that are absent in L^{T}_{TC}. The study of the pH-dependence of the Zn^{2+} binding constants shows that the metal ion is bound by four cysteinates above pH 5.2 and the binding constants are the highest reported so far. Interestingly, the binding constant of $Zn \cdot L_{TC}$ is about tenfold higher than that of $Zn \cdot L^{T}_{TC}$. This difference clearly indicates that the helix, present in $Zn \cdot L_{TC}$ only, stabilises the Zn^{2+} complex by about 1.2 kcal mol^{-1}. The

origin of this stabilisation is ascribed to an electrostatic interaction between the $[ZnS_4]^{2-}$ centre and the helix. This reveals a cooperative effect: zinc binding allows the folding of the tail into a helix which, in turn, strengthens the zinc complex.

- Tuning Nanostructure Morphology and Gold Nanoparticle "Locking" of Multi-Responsive Amphiphilic Diblock Copolymers.
  Smith, A. E.; Xu, X.; Abell, T. U.; Kirkland, S. E.; Hensarling, R. M.; McCormick, C. L. *Macromolecules* **2009**, *42*, 2958-2964.
  Abstract:

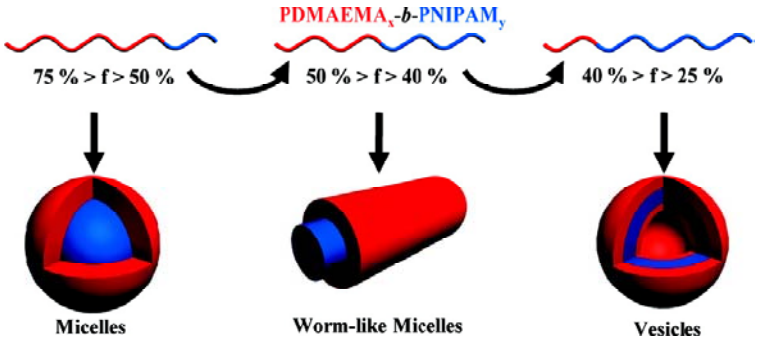

Reversible addition-fragmentation chain transfer (RAFT) polymerization was utilized to prepare multiresponsive, self-assembling amphiphilic poly[(*N*,*N*-dimethylaminoethyl methacrylate)$_x$-*b*-(*N*-isopropylacrylamide)$_y$] (DMAEMA$_x$-*b*-NIPAM$_y$). Controlling block lengths, solution pH, and NaCl concentration to elicit changes in the hydrophilic mass fraction resulted in specific morphological changes upon thermally induced assembly. At *y* = 102 (68 wt % DMAEMA), DMAEMA$_{165}$-*b*-NIPAM$_{102}$ copolymers self-assemble into simple core−shell micelles (58 nm). Increasing y to 202 (48 wt % DMAEMA) leads to a mixture of spherical micelles (78 nm) and worm-like micelles (*D* = 50−100 nm, *L* = 400−500 nm). Further increasing y to 435 (36 wt % DMAEMA) produces vesicular structures (179 nm). Significantly, reversible assembly of these nanostructures from the present stimuli-responsive diblock copolymers can be accomplished directly in aqueous media without the necessity of dialysis or manipulation with cosolvents. Additionally, the associated nanostructures can be shell cross-linked above the critical aggregation temperature *via* the *in situ* formation of gold nanoparticles yielding assemblies with long-term aqueous stability.

- Lower Critical Solution Temperature Behavior of Comb and Graft Shaped Poly[oligo(2-ethyl-2-oxazoline)methacrylate]s.
  Weber, C.; Becer, C. R.; Hoogenboom, R.; Schubert, U. S. *Macromolecules* **2009**, *42*, 2965-2971.
  Abstract:

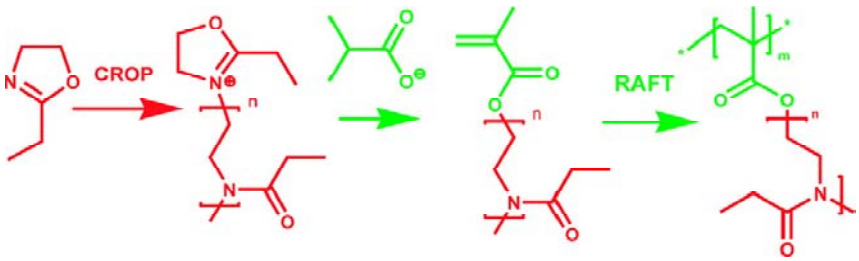

Comb and graft polymers with lower critical solution temperature (LCST) behavior based on hydrophilic oligo(2-ethyl-2-oxazoline) side chains and a hydrophobic methacrylate backbone were synthesized using the macromonomer method. Well-defined oligo(2-ethyl-2-oxazoline) methacrylate

(OEtOxMA) macromonomers were obtained by direct end-capping of living oligo(2-ethyl-2-oxazoline) chains with in situ formed triethylammonium methacrylate. The macromonomers were subsequently polymerized in a controlled manner using the reversible addition−fragmentation chain transfer (RAFT) polymerization technique yielding a series of comb polymers with varying side chain length and backbone length. In addition, a series of graft copolymers were prepared by copolymerizing OEtOxMA with methyl methacrylate (MMA, 40−80 mol %). The copolymers were characterized by ^{1}H NMR spectroscopy, size exclusion chromatography (SEC), and, partially, by matrix-assisted laser desorption ionization (MALDI-TOF) mass spectrometry. The LCST behavior of aqueous polymer solutions was investigated by turbidity measurements revealing cloud points that can be tuned from 35 to 80°C by variation of the MMA content.

- A Self-Sorting Scheme Based on Tetra-Urea Calix[4]arenes
  Rudzevich, Y.; Rudzevich, V.; Klautzsch, F.; Schalley, C. A.; Bohmer, V. *Angew. Chem. Int. Ed*. **2009,** *48*, 3867 –3871.
  Abstract:

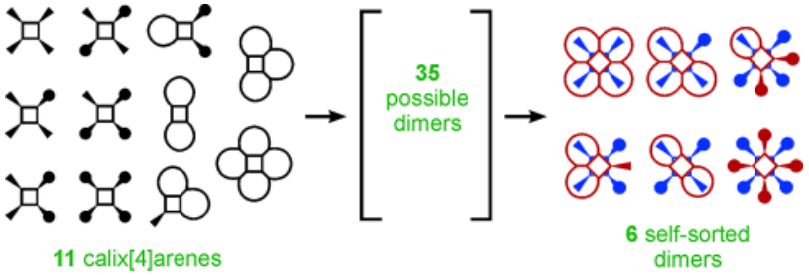

Size and shape do matter: When dimerized in nonpolar solvents, an equimolar mixture of eleven tetra-urea calix[4]arenes with different wide-rim substituents self-sorts into only six out of 35 different homo- and heterodimers (see picture). Since the calixarene scaffold and the four urea units are the same in all cases, the self-sorting process is driven only by the cooperative action of steric requirements and stoichiometry.

- Synthesis of Supramolecular Nanocapsules Based on Threading of Multiple Cyclodextrins over Polymers on Gold Nanoparticles
  Wu, Y.-L.; Li, J. *Angew. Chem. Int. Ed*. **2009,** *48*, 3842 –3845.
  Abstract:

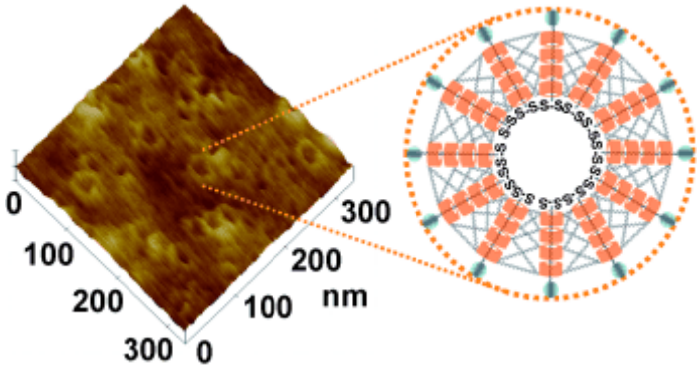

The CD's stuck: Poly(ethylene glycol) chains anchored onto gold nanoparticles (AuNPs) are threaded by multiple α-cyclodextrin (α-CD) rings to form a supramolecular outer layer composed of pseudopolyrotaxane columns perpendicular to the nanoparticle surface. Capping the polymer ends

confines α-CD on the nanoparticle surface, cross-linking the α-CD rings and then removing the AuNP cores produces supramolecular nanocapsules.

- Synthetic and structural studies on syringolin A and B reveal critical determinants of selectivity and potency of proteasome inhibition
  Clerc, J.; Groll, M.; Illich, D. J.; Bachmann, A. S.; Huber, R.; Schellenberg, B.; Dudler, R.; Kaiser, M. *Proc. Nat. Acad. Sci.* **2009**, *106*, 6507–6512.
  Abstract:

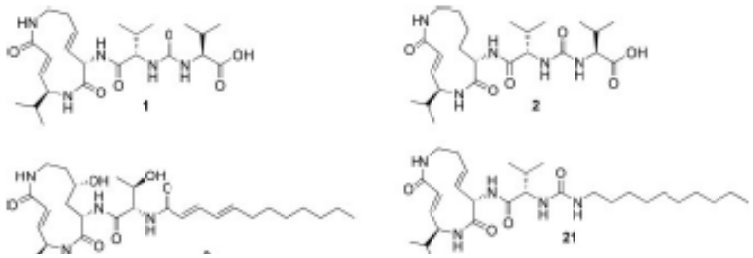

Syrbactins, a family of natural products belonging either to the syringolin or glidobactin class, are highly potent proteasome inhibitors. Although sharing similar structural features, they differ in their macrocyclic lactam core structure and exocyclic side chain. These structural variations critically influence inhibitory potency and proteasome subsite selectivity. Here, we describe the total synthesis of syringolin A and B, which together with enzyme kinetic and structural studies, allowed us to elucidate the structural determinants underlying the proteasomal subsite selectivity and binding affinity of syrbactins. These findings were used successfully in the rational design and synthesis of a syringolin A-based lipophilic derivative, which proved to be the most potent syrbactinbased proteasome inhibitor described so far. With a *K*_i of 8.65 _ 1.13 nM for the chymotryptic activity, this syringolin A derivative displays a 100-fold higher potency than the parent compound syringolin A. In light of the medicinal relevance of proteasome inhibitors as anticancer compounds, the present findings may assist in the rational design and development of syrbactin-based chemotherapeutics.

- Rapid sensitive analysis of cysteine rich peptide venom components
  Ueberheide, B. M.; Fenyö, D.; Alewood, P. F.; Chait, B. T. *Proc. Nat. Acad. Sci.* **2009**, *106*, 6910–6915.
  Abstract:

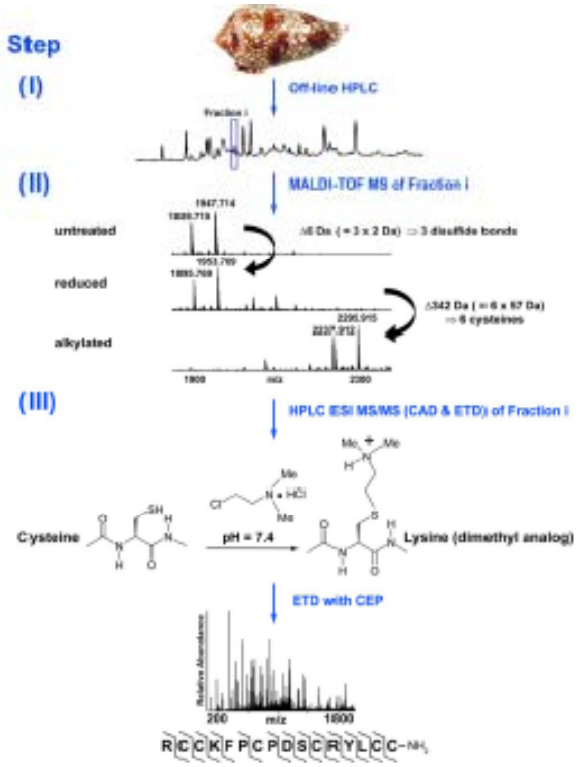

Disulfide-rich peptide venoms from animals such as snakes, spiders, scorpions, and certain marine snails represent one of nature's great diversity libraries of bioactive molecules. The various species of marine cone shells have alone been estimated to produce >50,000 distinct peptide venoms. These peptides have stimulated considerable interest because of their ability to potently alter the function of specific ion channels. To date, only a small fraction of this immense resource has been characterized because of the difficulty in elucidating their primary structures, which range in size between 10 and 80 aa, include up to 5 disulfide bonds, and can contain extensive posttranslational modifications. The extraordinary complexity of crude venoms and the lack of DNA databases for many of the organisms of interest present major analytical challenges. Here, we describe a strategy that uses mass spectrometry for the elucidation of the mature peptide toxin components of crude venom samples. Key to this strategy is our use of electron transfer dissociation (ETD), a mass spectrometric fragmentation technique that can produce sequence information across the entire peptide backbone. However, because ETD only yields comprehensive sequence coverage when the charge state of the precursor peptide ion is sufficiently high and the *m*/*z* ratio is low, we combined ETD with a targeted chemical derivatization strategy to increase the charge state of cysteine-containing peptide toxins. Using this strategy, we obtained full sequences for 31 peptide toxins, using just 7% of the crude venom from the venom gland of a single cone snail (*Conus textile*).

- Design of protein-interaction specificity gives selective bZIP-binding peptides
  Grigoryan, G.; Reinke, A. W.; Keating, A. E. *Nature* **2009**, *458*, 859-865.
  Abstract:

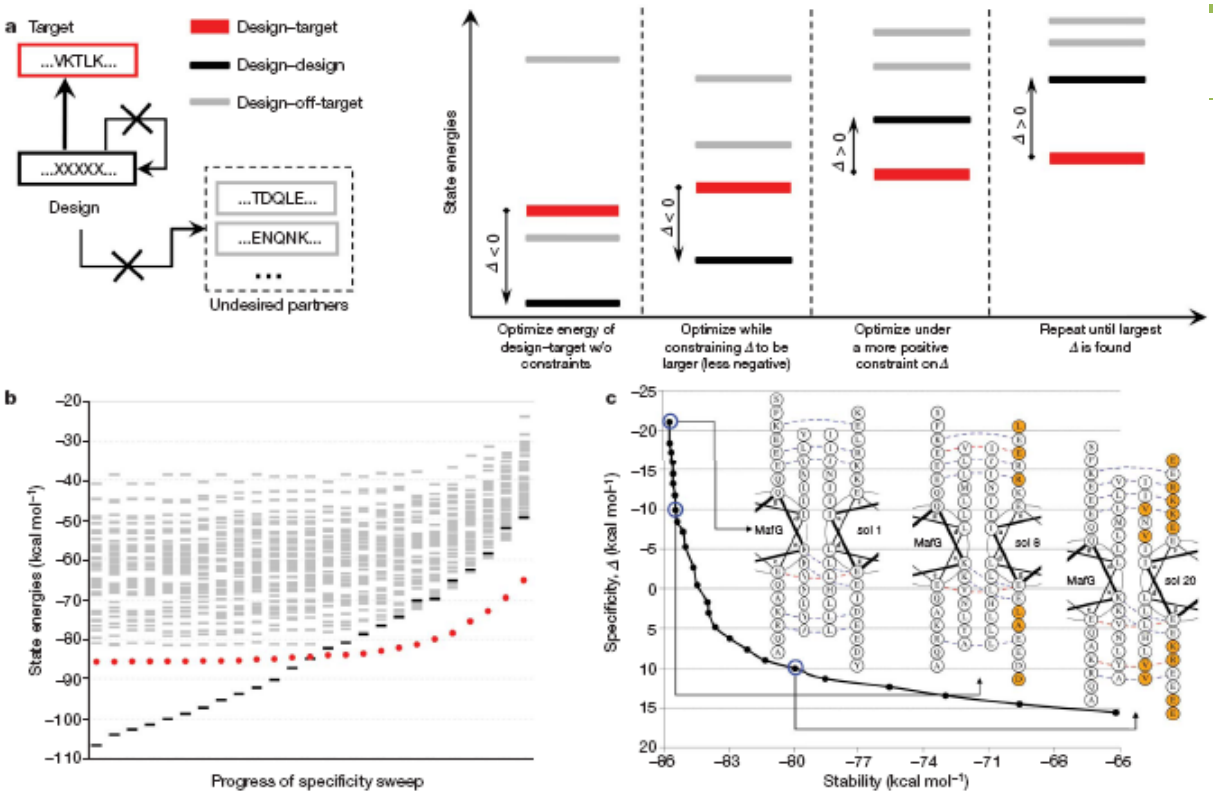

Interaction specificity is a required feature of biological networks and a necessary characteristic of protein or small-molecule reagents and therapeutics. The ability to alter or inhibit protein interactions selectively would advance basic and applied molecular science. Assessing or modelling interaction specificity requires treating multiple competing complexes, which presents computational and experimental challenges. Here we present a computational framework for designing protein-interaction specificity and use it to identify specific peptide partners for human basic-region leucine zipper (bZIP) transcription factors. Protein microarrays were used to characterize designed, synthetic ligands for all but one of 20 bZIP families. The bZIP proteins share strong sequence and structural similarities and thus are challenging targets to bind specifically. Nevertheless, many of the designs, including examples that bind the oncoproteins c-Jun, c-Fos and c-Maf (also called JUN, FOS and MAF, respectively), were selective for their targets over all 19 other families. Collectively, the designs exhibit a wide range of interaction profiles and demonstrate that human bZIPs have only sparsely sampled the possible interaction space accessible to them. Our computational method provides a way to systematically analyse trade-offs between stability and specificity and is suitable for use with many types of structure-scoring functions; thus, it may prove broadly useful as a tool for protein design.